Exploring the comorbidity mechanism of rheumatoid arthritis and systemic lupus erythematosus through transcriptomics and conducting experimental validation

M. Shen, C. You

[1]*Laboratory Medical Center, Lanzhou University Second Hospital, Lanzhou, China.*

Abstract

Objective

Rheumatoid arthritis (RA) and systemic lupus erythematosus (SLE) are two systemic autoimmune diseases with significant comorbidity, and the shared molecular mechanisms remain unclear.

Methods

This study integrates four transcriptomic datasets (GSE17755, GSE110169, GSE93272, GSE110174), combining differential expression gene (DEG) screening, protein-protein interaction (PPI) network analysis, machine learning (LASSO and random forest), and single-sample gene set enrichment analysis (ssGSEA) to systematically analyse the comorbidity mechanisms of RA and SLE.

Results

It was found that RA and SLE share immune regulatory genes such as IFIT3, TNFSF13B, and ZCCHC2, which are significantly upregulated in both diseases and have high diagnostic efficacy. Functional analysis shows that IFIT3 is associated with type I interferon and cGAS-STING pathways, TNFSF13B (BAFF) is associated with B cell activation and TLR signalling pathways, and ZCCHC2 is associated with cell cycle regulation and neurodegenerative diseases. Immune cell analysis indicates that in RA, macrophages are positively correlated with TNFSF13B, while in SLE, plasmacytoid dendritic cells (pDCs) are negatively correlated with IFIT3, suggesting disease-specific differences in the immune microenvironment.

Conclusion

This study elucidates the molecular mechanisms of RA and SLE comorbidity, identifies cross-disease biomarkers and their interactions with immune cells and drugs, providing theoretical basis for precision diagnosis and treatment. The study limitations include data heterogeneity and the lack of Rhupus patient samples, which need to be validated through functional experiments and multicentre cohorts in the future.

Key words

rheumatoid arthritis, systemic lupus erythematosus, comorbidity mechanisms, machine learning

Minghui Shen, MD
Chongge You, MD

Please address correspondence to:
Chongge You
Laboratory Medical Center,
Lanzhou University Second Hospital,
no. 82 Cuiying Gate, Linxia Road,
Chenguan District,
Lanzhou 730030,
Gansu Province, China.
E-mail: youchg@lzu.edu.cn

Received on June 10, 2025; accepted in revised form on October 9, 2025.

Funding: Gansu Province Natural Science Foundation (grant no. 21JR1RA173) and Lanzhou Science and Technology Project (grant no. 2020-ZD-90).

Competing interests: none declared.

Introduction

Rheumatoid arthritis (RA) is a systemic autoimmune disease characterised by chronic synovitis and joint destruction, with a global prevalence of approximately 0.5–1%, and a female-to-male incidence ratio of 2-3:1 (1-3). Its pathogenesis involves genetics, environment (such as smoking) and abnormal activation of the immune system, especially the release of pro-inflammatory cytokines (such as TNF-α and IL-6) mediated by T cells, B cells and macrophages, leading to synovial hyperplasia and bone erosion (4-6). Despite the identification of multiple risk loci through genome-wide association studies (GWAS), such as HLA-DRB1, the molecular mechanisms of rheumatoid arthritis (RA) are still not fully elucidated (7). In recent years, bioinformatics analysis has revealed the key roles of immune-related genes (such as STAT3 and the JAK-STAT pathway) and immune cell infiltration (such as Th17 cells) in the progression of RA through the mining of transcriptomic data (5, 8, 9).

SLE is a systemic autoimmune disease characterised by multi-organ involvement (such as skin, kidneys, and cardiovascular system) and the formation of autoantibodies, with a prevalence of approximately 20–150 cases per 100,000 people, and a female predominance of up to 90% (3, 10, 11). Its pathogenesis is closely related to the deposition of immune complexes (such as anti-dsDNA antibodies), over-activation of type I interferon signalling pathways, and B cell dysfunction (10, 12, 13). Genetic studies show that SLE is associated with polymorphisms in genes such as IRAK1 and STAT4, but the comorbidity mechanisms with other autoimmune diseases (such as RA) still need to be further explored (7, 11). Transcriptomic analysis indicates that interferon stimulated genes (ISGs) and Toll-like receptor (TLR) pathways are significantly upregulated in peripheral blood mononuclear cells (PBMCs) of SLE patients, suggesting an aberrant innate immune response in the disease (12, 14).

RA and SLE co-morbidity mechanism: clinical and epidemiological studies have shown that RA and SLE can co-occur (such as in Rhupus syndrome), with some patients exhibiting features of both diseases (15, 16). Rhupus syndrome is a rare autoimmune disease that combines features of RA and SLE. Its clinical manifestations include: 1. symmetric erosive polyarthritis (similar to RA), often accompanied by joint deformities and morning stiffness; 2. skin manifestations (such as photosensitive rashes, hair loss), haematological abnormalities (such as pancytopenia), pleuritis, and renal involvement (with an incidence of about 10%, lower than the 25% seen in typical SLE) (17, 18).

Genetic evidence shows that both share some risk loci (such as the HLA region) and immune pathways (such as the JAK-STAT and TLR signalling pathways) (7, 13). Additionally, bioinformatics analysis revealed that comorbidity between RA and SLE may be associated with similarities in common differentially expressed genes (such as CXCL10, IFI44L) and immune microenvironment (such as neutrophil infiltration) (13, 14, 19). However, systematic studies of these shared molecular mechanisms are still insufficient, especially those based on transcriptomic data across diseases.

This study aims to identify key genes, pathways, and immune cell infiltration patterns shared by RA and SLE by integrating bulk RNA-seq data from both conditions using bioinformatics methods. We hypothesise that RA and SLE share transcriptional regulatory networks and immunological dysregulation mechanisms, which may provide new insights for diagnostic biomarkers or therapeutic targets for these diseases. By systematically comparing the molecular characteristics of the two diseases, this study will fill gaps in the understanding of comorbidity mechanisms and provide theoretical support for precision medicine strategies.

The aim of this study is to explore the possible shared molecular mechanisms between RA and SLE by integrating transcriptomic data analysis, machine learning model construction, and multiple bioinformatics and experimental validation methods. Figure 1 details the entire research process from raw data set processing, identification of DEGs,

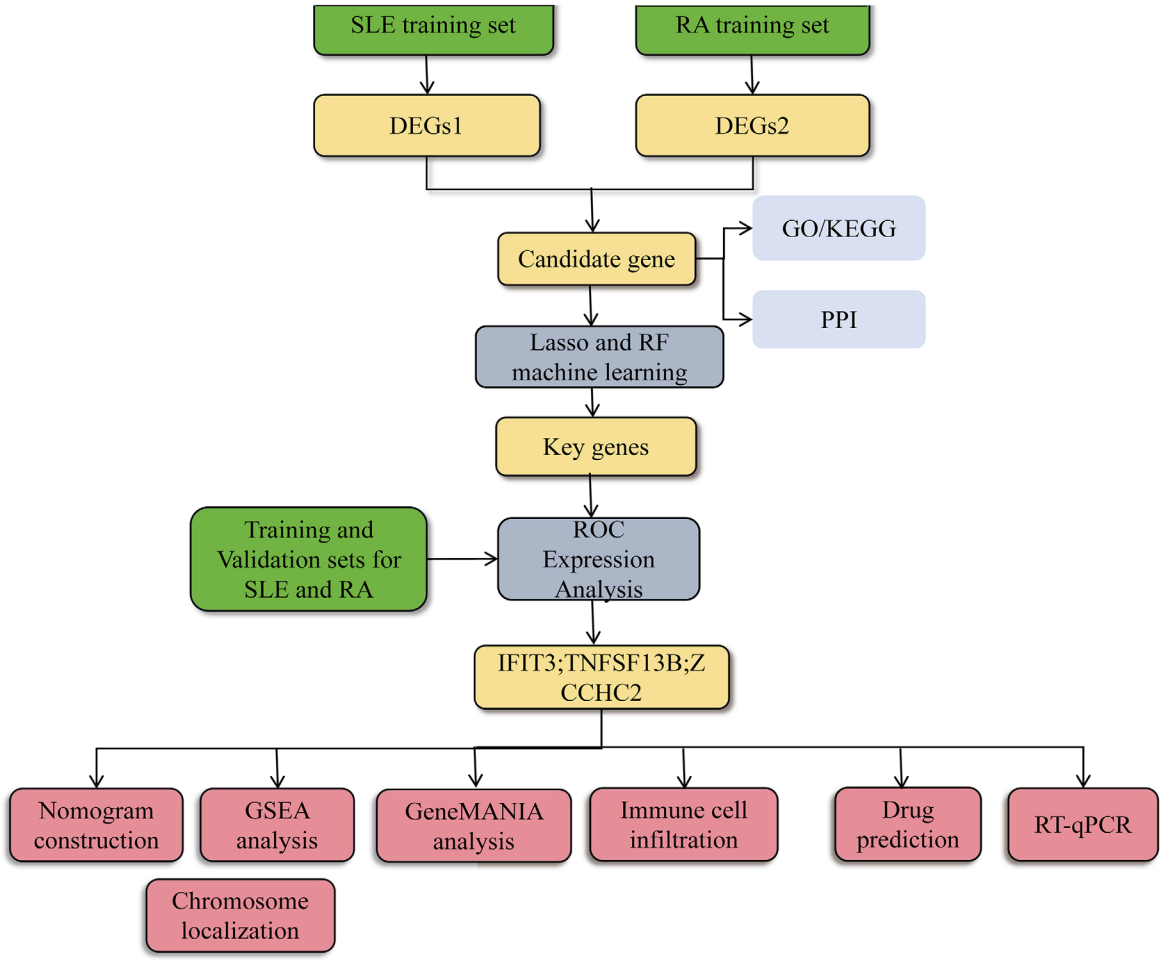

Fig. 1. The framework of multi-omics integrated analysis was used to analyse the key genes of SLE and RA. In this study, we identified key genes common to SLE and RA through integrated multiomics analysis. Firstly, differential genes were screened based on GSE110169 (SLE) and GSE17755 (RA) datasets to obtain candidate genes. Through functional enrichment analysis, protein interaction network and machine learning screening, key genes were finally identified, and finally gene expression was verified by qPCR experiment.

screening of key genes, diagnostic efficacy assessment, and subsequent functional analysis, drug prediction, and experimental validation. The core goal of the study is to identify key genes of diagnostic value shared by RA and SLE, and further reveal their potential functions and molecular roles in disease development (Fig. 1).

Materials and methods

Acquisition and preprocessing of microarray data

The expression datasets for RA and SLE, GSE17755, GSE110169, GSE93272, and GSE110174, were downloaded from NCBI GEO (http://www.ncbi.nlm.nih.gov/geo/, access time: 2025/05/01). Among them, GSE17755 and GSE110169 were used as the training set, while GSE93272 and GSE110174 were used as the test set. Subsequently, the datasets were preprocessed using the R package limma to obtain differentially expressed genes. After setting the parameters adj.*p*-value <0.05 and |logFC| ≥1.5 to limit the data, data visualisation was performed using the R package ggplot2. Then, the R package VennDiagram (1.7.3) was used to obtain the intersection of DEGs between RA and SLE.

For the training set GSE17755 and GSE110169, gene expression profiling was conducted on peripheral blood cells from patients with autoimmune diseases. GSE177755 includes 112 patients with RA, 22 patients with SLE, 6 patients with polyarticular juvenile idiopathic arthritis (polyJIA), 51 patients with systemic juvenile idiopathic arthritis (sJIA), 8 healthy children, and 45 healthy adults. In this study, 112 RA patients were included as the disease group and 59 healthy individuals as the control group. For the training set GSE110169, it includes 82 SLE patients, 84 RA patients, and 77 healthy controls. In this study, 82 SLE patients were included as the disease group and 77 healthy individuals as the control group. For the validation set GSE93272, it includes 43 samples from healthy controls and 233 RA samples; the validation set GSE110174 includes 10 samples from healthy controls and 144 SLE samples, used for expression profiling validation.

Screening and enrichment analysis of overlapping genes between RA and SLE

To further identify overlapping genes between RA and SLE, the intersection of upregulated and downregulated genes in RA and SLE was combined

to obtain the overlapping genes. These overlapping genes were further used for enrichment analysis. Then, we performed gene ontology (GO) annotation and Kyoto Encyclopedia of Genes and Genomes (KEGG) pathway enrichment analysis using R language. The GO analysis included cellular component, biological process, and molecular function. A protein-protein interaction (PPI) network of these overlapping genes was constructed using the STRING online tool (confidence >0.4) (https://string-db.org/cgi/input.pl, access time: 2025/05/01).

Construction of machine learning models

In GSE17755, LASSO analysis was conducted on candidate genes using the R package glmnet (4.1-8) with 10-fold cross-validation to select the optimal lambda (λ) value for gene selection. Random forest analysis was then performed on the candidate genes using the R package randomForest (4.7-1.2) with 10-fold cross-validation to further screen the genes. Finally, the R package VennDiagram (1.7.3) was used to find the intersection of genes selected by both algorithms, which were designated as key genes 1. In GSE110169, the same algorithms were applied to obtain key genes 2. Ultimately, the intersection of key genes 1 and key genes 2 was determined using the R package VennDiagram (1.7.3) and defined as potential biomarkers.

LASSO achieves feature sparsity through L1 regularisation, effectively screening key variables in high-dimensional data (such as clinical features or genetic markers), while random forests handle non-linear relationships through ensemble decision trees and assess feature importance. Some studies suggest that this combination "combines the advantages of LASSO regression and ensemble strategies", both improving the stability of variable selection through LASSO and utilising random forests to capture complex interactions (20-22). Ding *et al*. proposed the Collaborative Regularisation Linear Regression framework, combining the LASSO penalty term with ensemble methods to maintain feature sparsity while improving prediction accuracy (23). Ouyang *et al*. further verified that by pre-screening features with LASSO and then inputting them into models such as random forest, the accuracy of prognostic prediction can be significantly improved (24). The combination is widely used for disease risk prediction (such as diabetes, cancer) and biomarker discovery, both of which adopt 10-fold cross-validation for hyperparameter optimisation and model evaluation. Its advantage lies in balancing computational efficiency and data utilisation (25).

ROC analysis

To evaluate the discriminative power of the key genes obtained in the previous step for patient samples and control samples, ROC curve analysis was performed on the key genes in the training and validation sets of RA and SLE using the R package pROC (1.18.5) to calculate the Area Under the Curve (AUC) values.

Level of expression analysis

To investigate the expression levels of the potential biomarkers obtained in RA and SLE patient samples and control samples, the Wilcoxon rank-sum test was used to analyse the expression levels of the potential biomarkers ($p<0.05$).

Nomogram construction

Nomogram diagram, which is based on multi-factor regression analysis, integrates multiple prediction indexes, and then draws them on the same plane according to a certain scale by using line segments with scales, so as to express the relationship between variables in the prediction model. The basic principle is to assign a score to each value level of each influencing factor according to the contribution degree of each influencing factor to the outcome variable (the size of regression coefficient) in the model, and then add up all scores to obtain the total score. Finally, the predictive value of the individual outcome event is calculated through the function transformation relationship between the total score and the occurrence probability of the outcome event. The nomogram transforms complex regression equations into visual graphs, making the results of predictive models more readable and convenient for patient assessment. Because of its intuitionistic and easy-to-understand characteristics, nomogram has gradually gained more and more attention and application in medical research and clinical practice.

The genes with ROC >0.7 and consistent expression trends in RA and SLE patient samples and control samples were determined as final biomarkers. A nomogram was constructed for biomarkers using the R package rms (6.8-1). Each biomarker corresponds to a score. The total score of each biomarker corresponds to the total score. The risk of disease was predicted according to the total score. The higher the total score, the higher the risk of disease.

Chromosome mapping and GeneMANIA analysis

Chromosomal localisation of genes is of great significance to the study of gene structure, function and interaction. In order to explore the chromosomal localisation of biomarkers, the R package RCircos (1.2.2) was used to visualise their chromosomal localisation.

Gene set enrichment analysis

In this study, in order to explore the functional enrichment of markers, Spearman correlation between biomarkers and all other genes was calculated by R package psych (2.4.6.26) in all samples of training set, and ranked from large to small according to correlation coefficient, and then GSEA enrichment analysis was performed by R package clusterProfiler (4.15.0.003). The reference gene set was c2.all.v2024.1.Hs.symbols.gmt of MSigDB database (https://www.gsea-msigdb.org/gsea/msigdb, access time: 2025/05/05), and the screening threshold was $p<0.05$ and $|NES|>1$.

Immune cell infiltration

In order to explore the correlation between biomarkers and immune cells in RA and SLE, and to understand the composition of immune cells, we used single sample gene enrichment analysis (ssGSEA) to analyse immune infiltration correlation analysis. The R pack-

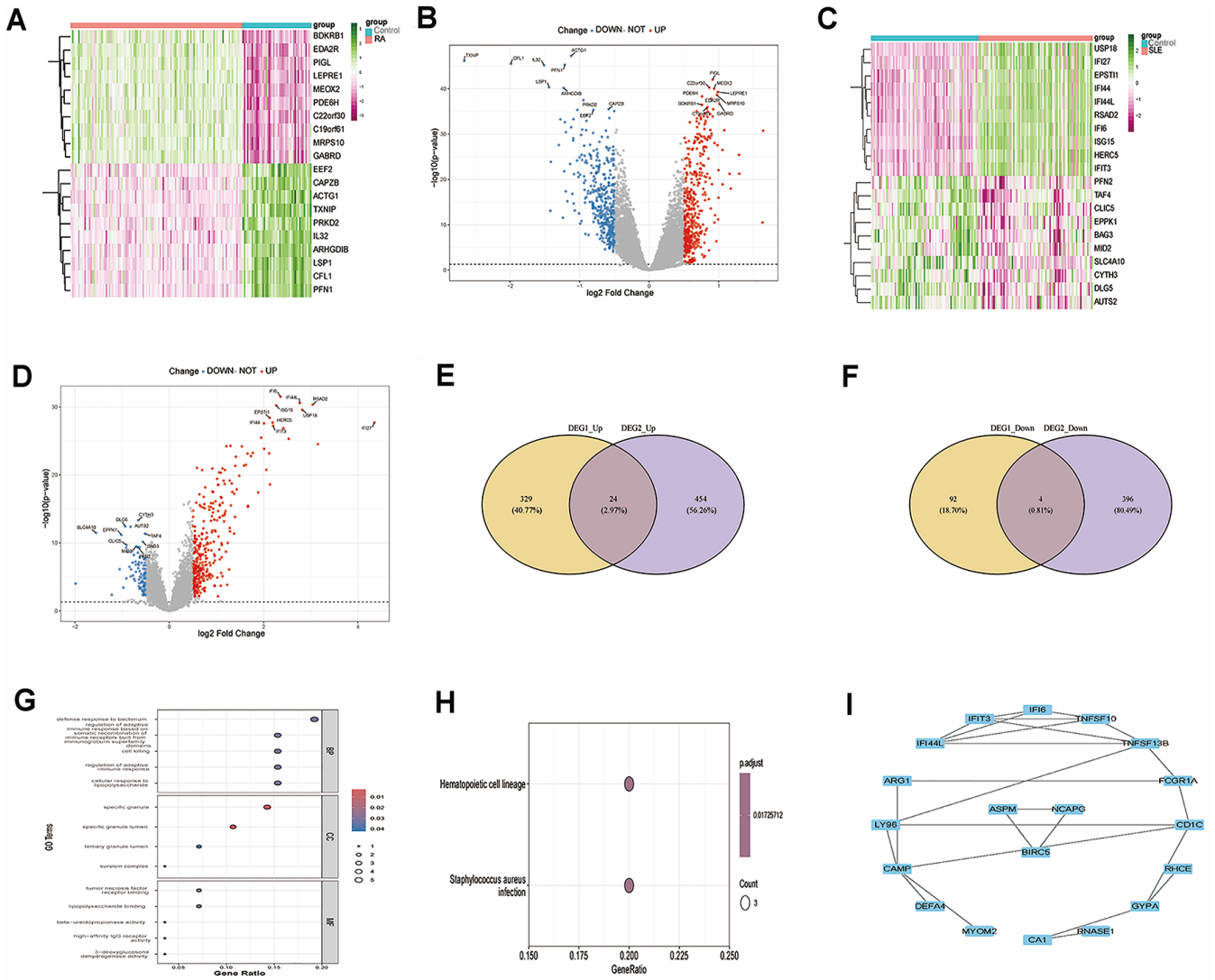

Fig. 2. Expression spectrum characteristics of GSE17755 and GSE110169.
A: The expression spectrum heat map of the GSE17755 data set, the red part is the RA group and the blue part is the Control group; **B**: For the volcano map of the GSE17755 data set, select the top 10 genes to display (the threshold value is adj.*p*-value <0.05&log|FC|≥1.5); **C**: The expression spectrum heat map of the GSE110169 data set, the red part is the SLE group and the blue part is the Control group; **D**: The volcano map of the GSE110169 data set, select the top 10 genes to display (the threshold value is adj.*p*-value <0.05&log|FC|≥1.5; **E**: Intersection of upregulated genes in GSE17755 and GSE110169 data sets; **F**: Intersection of downregulated genes in GSE17755 and GSE110169 data sets; **G**: The intersecting genes in E and F are taken and merged for GO enrichment analysis; **H**: The intersecting genes in E and F are taken and merged for KEGG enrichment analysis; **I**: After the intersection genes in E and F are taken and merged, the ppi network diagram is drawn and visualised.

age GSVA (1.53.28) was used to calculate enrichment scores for disease and normal samples in 28 immune cells.

Analysis of the association between biomarkers and diseases

In order to find other diseases that may be associated with biomarkers, the DisGeNet database (http://www.disgenet.org/, access time: 2025/05/09) was used to screen for diseases associated with biomarkers, ker-disease relationships were examined by NetworkAnalyst (https://www.networkanalyst.ca/, access time: 2025/05/11), ker-associated diseases and their complications were revealed based on the DiGeNET database, and finally ker-disease co-expression networks were visualised with R package enrichplot (1.20.0).

RT-QPCR experimental validation

Peripheral blood mononuclear cell (PBMC) samples were collected from clinically confirmed RA patients (n=30), SLE patients (n=30) and healthy controls (n=30). All samples were collected from active patients, approved by the hospital ethics committee and signed informed consent form. ΔΔCt method was used to calculate the relative expression, and GAPDH was used as internal reference gene. Differences between groups were analysed by ANOVA and Tukey's *post-hoc* test with $p<0.05$ and Cohen's $d>0.5$.

RA patients (n=30), SLE patients (n=30), and healthy controls (n=30) showed no significant differences in age (mean±SD: RA 43.2±11.8 years, SLE 41.5±10.3 years, control 44.1±9.7 years, ANOVA $p=0.62$) and gender distribution (female percentage: RA 83.3%, SLE 86.7%, control 80.0%, Chi-square test $p=0.78$). All patients

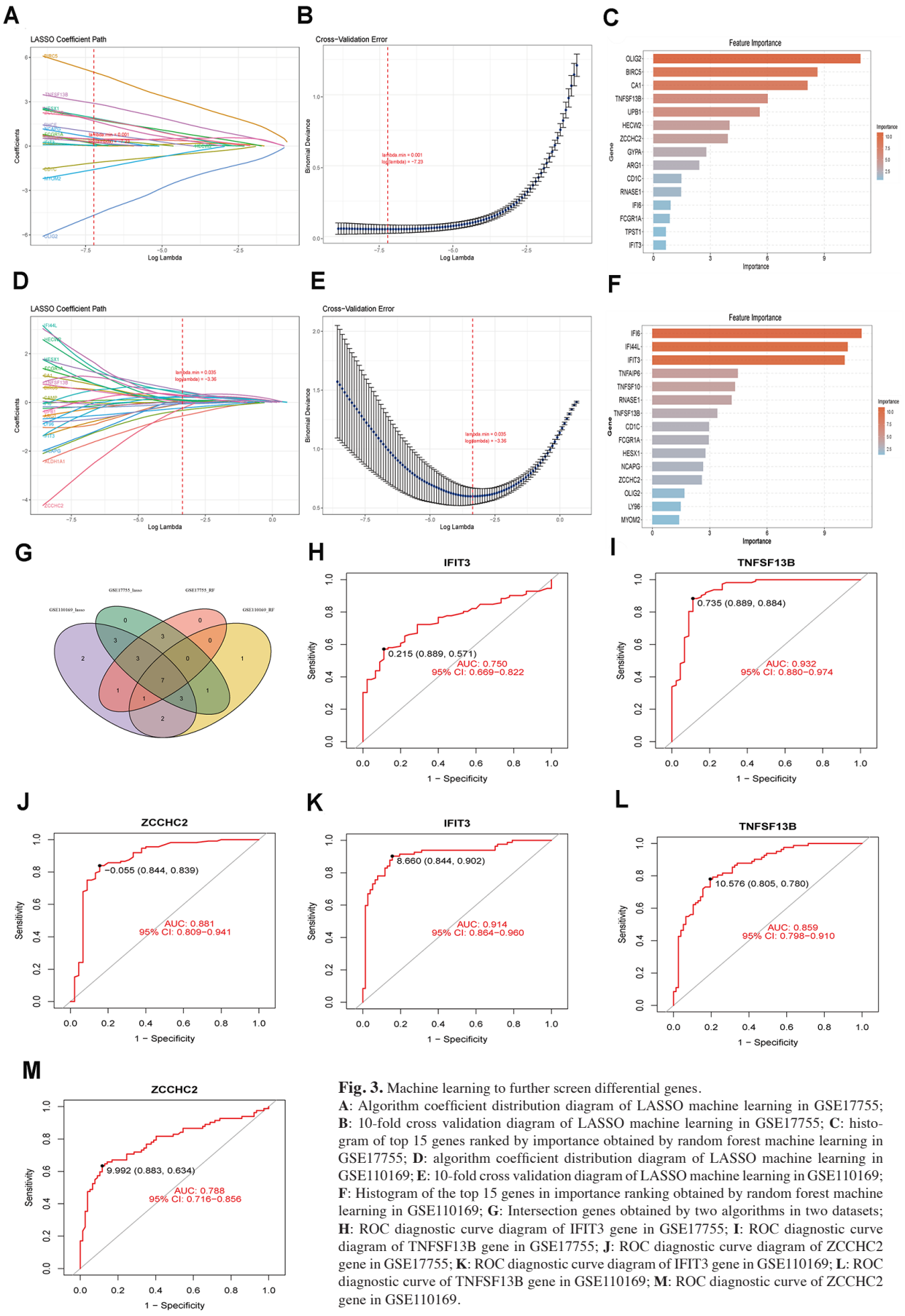

Fig. 3. Machine learning to further screen differential genes.
A: Algorithm coefficient distribution diagram of LASSO machine learning in GSE17755; **B**: 10-fold cross validation diagram of LASSO machine learning in GSE17755; **C**: histogram of top 15 genes ranked by importance obtained by random forest machine learning in GSE17755; **D**: algorithm coefficient distribution diagram of LASSO machine learning in GSE110169; **E**: 10-fold cross validation diagram of LASSO machine learning in GSE110169; **F**: Histogram of the top 15 genes in importance ranking obtained by random forest machine learning in GSE110169; **G**: Intersection genes obtained by two algorithms in two datasets; **H**: ROC diagnostic curve diagram of IFIT3 gene in GSE17755; **I**: ROC diagnostic curve diagram of TNFSF13B gene in GSE17755; **J**: ROC diagnostic curve diagram of ZCCHC2 gene in GSE17755; **K**: ROC diagnostic curve diagram of IFIT3 gene in GSE110169; **L**: ROC diagnostic curve of TNFSF13B gene in GSE110169; **M**: ROC diagnostic curve of ZCCHC2 gene in GSE110169.

were in the active phase (RA: DAS28-CRP≥3.2; SLE: SLEDAI≥6), receiving standard treatment protocols (hormone/immunosuppressant use rate >80%).

Statistical analysis

- Differentially DEG analysis

DEG analysis was performed using the limma package (3.56.2) of the R language. The original expression matrix is first transformed log2 (PKM+1). Linear models were then constructed for each dataset (GSE110169, GSE17755, GSE93272). Apply empirical Bayesian adjustment through the eBayes function and output the results using the topTable function. The adj.*p*-value column of the topTable function output represents the *p*-value corrected for multiple tests (FDR) by the Benjamini-Hochberg (BH) method. We set adj.*p*-value <0.05 and |log2 FC| Genes >1.5 were defined as differentially expressed genes with statistical significance.

- ROC curve evaluation

To evaluate the diagnostic value of key genes (IFIT3, TNFSF13B, etc.) in distinguishing patients from controls, we separately plotted receiver operating characteristic (ROC) curves for each gene in two independent datasets (GSE110169 and GSE17755) and calculated the following indicators: area under the curve (AUC): calculated using the pROC package, reflecting the overall discriminative ability of the gene; 95% confidence interval (CI): generated based on 1000 times of bootstrap sampling; significance test: for each gene's AUC, a one-sample test is performed against a random classifier (AUC=0.5) using the two-tailed Z-test (roc.test function); multiple test correction: the Benjamini-Hochberg (BH) method is used to control the false discovery rate (FDR), and corrected *p*-values (q-values) <0.05 are considered significant.

- Immune cell correlation analysis

To explore the potential association between IFIT3, TNFSF13B, and ZCCHC2 genes and the infiltration scores of 28 immune cells, we calculated the Spearman rank correlation coefficient. This analysis was performed using the corr.test function from the psych R language package, and all calculated *p*-values were subjected to multiple testing correction using the Benjamini-Hochberg (BH) method via the adjust = fdr parameter. Only results with correlation coefficients and adjusted *p*-values <0.05 are reported.

- RT-qPCR experiment

To validate the expression differences of IFIT3, TNFSF13B, and ZCCHC2 genes in RA patients *versus* healthy controls and SLE patients *versus* healthy controls, we conducted RT-qPCR experiments. A total of 6 main comparisons were made. For each comparison, we used the Wilcoxon rank-sum test to evaluate the relative expression levels of the genes. To control for the multiple testing effects of these 6 comparisons, we applied the Benjamini-Hochberg (BH) method for FDR correction to all *p*-values. Adjusted *p*-values <0.05 were considered statistically significant.

Results

Explore DEGs between RA and SLE patient samples and control samples

Based on RA training set (GSE17755) and SLE training set (GSE110169), strict screening criteria (adj.*p*-value <0.05, |log2FC| ≥1.5) identify disease-specific differentially expressed genes. A total of 449 significant DEGs (353 up-regulated and 96 down-regulated) were identified in the RA cohort, with PIGL and ACTG1 as the most significant up-regulated and down-regulated genes, respectively (Fig. 2A-B). 878 DEGs were identified in the SLE cohort (478 up-regulated and 400 down-regulated), with IFI6 and SLC4A10 showing the most significant expression differences (Fig. 2C-D). Cross analysis revealed significant overlap in immune regulatory genes between RA and SLE: the intersection of up-regulated genes contained 24 key genes, and the intersection of down-regulated genes contained 4 genes (Fig. 2E-F). GO/KEGG enrichment analysis revealed that these shared genes are mainly involved in innate immune response and haematopoietic cell differentiation pathways, among which TNFSF13B, as a core regulator of B cell activation, is significantly upregulated in both diseases (Fig. 2G-H). PPI network constructed based on STRING database shows that the pivot genes IFIT3 and TNFSF13B may serve as molecular hubs for RA and SLE co-disease (Fig. 2I).

Identifying candidate pivot genes and ROC evaluation by machine learning

To screen candidate genes for nomogram construction and diagnostic value assessment, LASSO regression and RF machine learning algorithms were applied (Fig. 3A-F). In RA training set GSE17755, we selected the intersection of 19 genes identified by LASSO regression algorithm and the first 15 genes obtained by random forest algorithm as candidate biomarkers for RA. In SLE training set GSE110169, we took the intersection of 22 genes determined by LASSO regression algorithm and the first 15 genes obtained by random forest algorithm as candidate biomarkers for SLE, and obtained the intersection of four genes, totaling 7 genes, for subsequent verification (Fig. 3G). Meanwhile, ROC evaluation showed that AUC of IFIT3, TNFSF13B and ZCCHC2 were 0.750 (95%CI 0.669–0.822), 0.932 (95% CI 0.880–0.974) and 0.881 (95%CI 0.809–0.941) in RA (Fig. 3H-J). In SLE, AUC of IFIT3, TNFSF13B and ZCCHC2 were 0.914(95%CI 0.864–0.960), 0.859 (95% CI 0.789–0.910) and 0.788 (95%CI 0.716–0.856) (Fig. 3K-M).

Further screening and nomogram evaluation of candidate genes

To investigate the expression of the 7 potential biomarkers in RA and SLE patient samples and control samples, Wilcoxon rank sum test was used for RA and SLE training set and validation set (GSE17755, GSE110169, GSE93272, and GSE110174) were analysed ($p<0.05$), and genes significantly different and with consistent expression trends in both datasets were defined as biomarkers (IFIT3, TNFSF13B, ZCCHC2) (Fig. 4A-D).

The nomogram was constructed based on three candidate central genes and

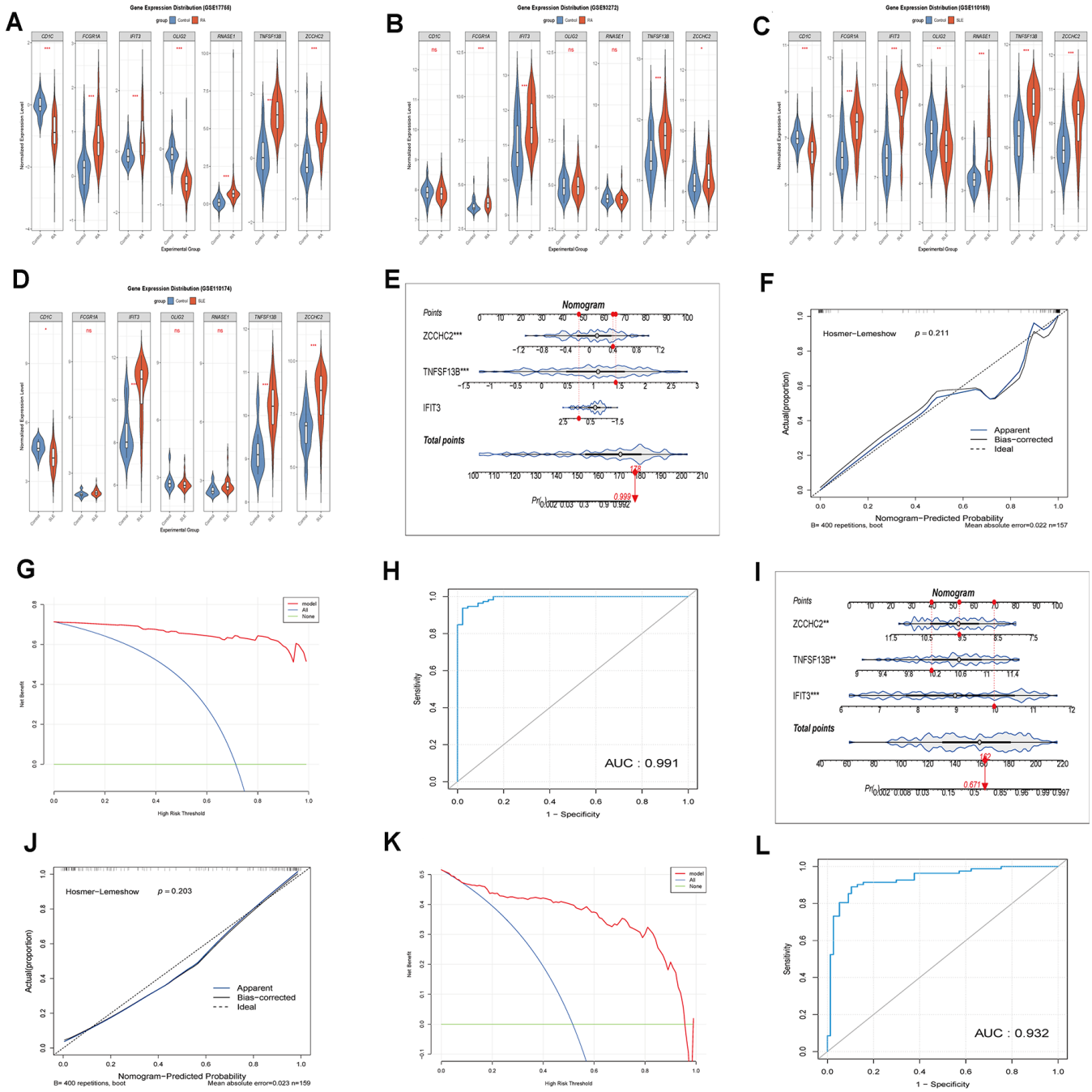

Fig. 4. Through validation datasets, key genes are further confirmed.
A: Violin plots of the expression of CD1C, FCGR1A, IFIT3, OLIG2, RNASE1, TNFSF13B, and ZCCHC2 genes in GSE17755; **B**: Violin plots of the expression of CD1C, FCGR1A, IFIT3, OLIG2, RNASE1, TNFSF13B, and ZCCHC2 genes in GSE93272; **C**: Violin plots of the expression of CD1C, FCGR1A, IFIT3, OLIG2, RNASE1, TNFSF13B, and ZCCHC2 genes in GSE110169; **D**: Violin plots of the expression of CD1C, FCGR1A, IFIT3, OLIG2, RNASE1, TNFSF13B, and ZCCHC2 genes in GSE110174; **E**: Calibration plots of the ZCCHC2, TNFSF13B, and IFIT3 genes in GSE17755; **F**: Calibration curve plot in GSE17755; **G**: DCA plot in GSE17755; **H**: ROC diagnostic curves of the ZCCHC2, TNFSF13B, and IFIT3 genes in GSE17755; **I**: Calibration plots of the ZCCHC2, TNFSF13B, and IFIT3 genes in GSE110169; **J**: Calibration curve plot in GSE110169; **K**: DCA plot in GSE110169; **L**: ROC diagnostic curves of the ZCCHC2, TNFSF13B, and IFIT3 genes in GSE110169.

ROC curves were established to assess the diagnostic specificity and sensitivity of these three gene sets and nomograms (Fig. 4E, H, I, L). We calculated AUC and 95% CI for each item. The results were as follows: RA (AUC 0.991, 95% CI 0.982–1.000), SLE (AUC 0.932, 95% CI 0.891–0.973) (Fig. 4H, L). These three genes have high diagnostic value for RA and SLE, and the nomogram constructed also has high diagnostic value (Fig. 4E, I).

In order to evaluate the prediction performance of nomogram models, calibration curves are often used to visually show the relationship between predicted probability values and true probability values. In RA, calibration curves were plotted using the rms package, p=0.221, indicating that the nomogram had better prediction accuracy; in SLE, p=0.203,

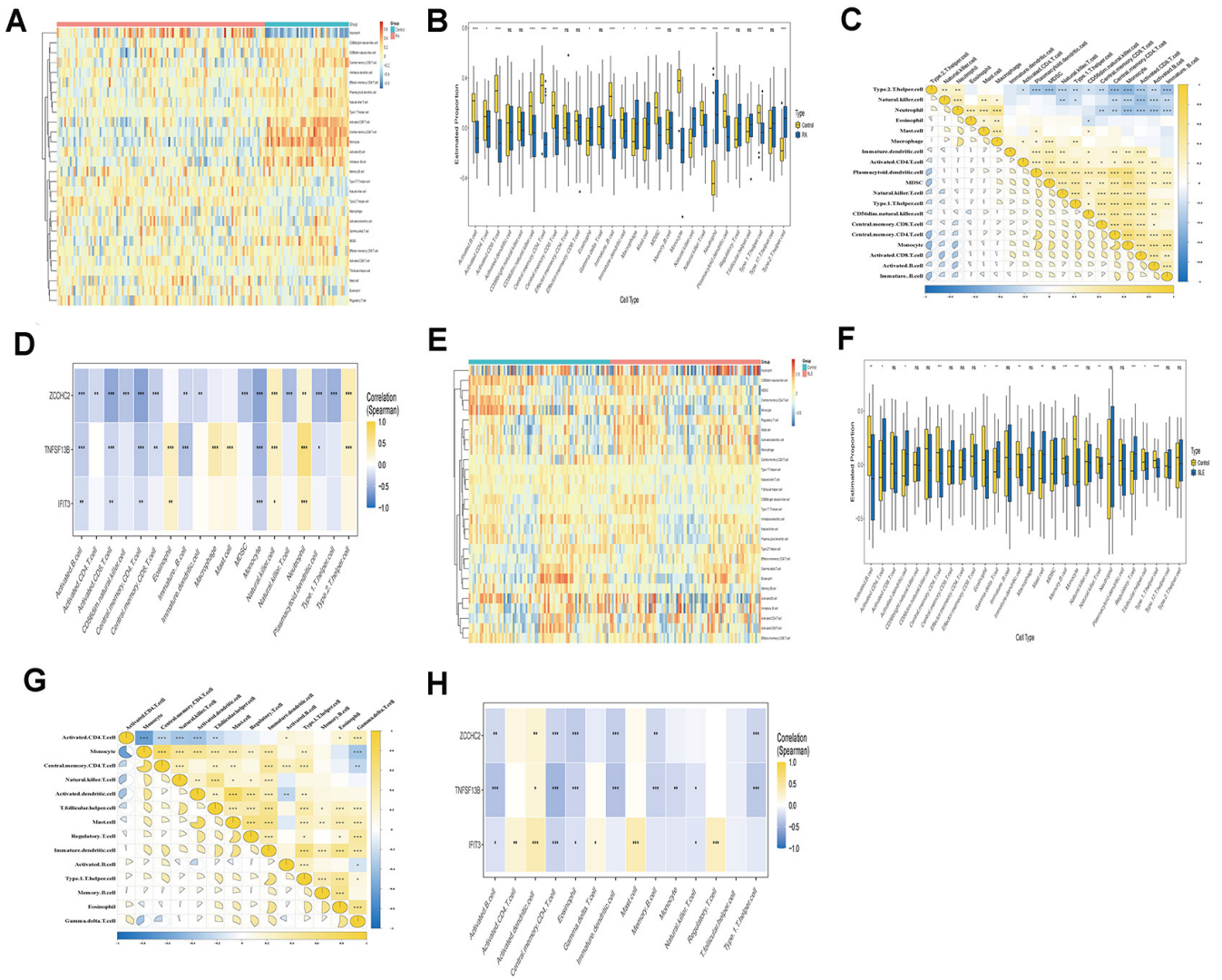

Fig. 5. Immune infiltration analysis.
A: Heatmap of expression of 28 immune cells in GSE17755; **B**: Bar chart of expression of 28 immune cells in GSE17755; **C**: Correlation analysis of differentially expressed immune cells in GSE17755; **D**: Correlation analysis of ZCCHC2, TNFSF13B, and IFIT3 with differentially expressed immune cells in GSE17755; **E**: Heatmap of expression of 28 immune cells in GSE110169; **F**: Bar chart of expression of 28 immune cells in GSE110169; **G**: Correlation analysis of differentially expressed immune cells in GSE110169; **H**: Correlation analysis of ZCCHC2, TNFSF13B, and IFIT3 with differentially expressed immune cells in GSE110169.

indicating that the nomogram had better prediction accuracy (Fig. 4F, J).

Decision curve (DCA) analysis was used to assess the clinical utility of the linear nomogram, and the R package rmda was used to draw the decision curve. It can be seen from the figure that the model curve has a certain distance from the two extreme curves and has a good prediction effect. Meanwhile, the net benefit rate of the nomogram is higher than that of other key genes, indicating that the prediction effect of the model is the best (Fig. 4G, K).

Immune cell infiltration analysis

This study systematically investigated the characteristics of immune cell composition and its correlation with key biomarkers in RA and SLE. Firstly, single-sample gene set enrichment analysis (ssGSEA) algorithm was used to calculate the infiltration score of 28 immune cell subsets by R software package GSVA (1.53.28), and the pheatmap (1.0.12) package was used to construct the immune cell abundance pheatmap of control group and disease group (Fig. 5A, E). The visualisation results showed that RA and SLE patients showed unique immune cell distribution patterns, suggesting that autoimmune diseases may trigger systemic immune microenvironment remodelling.

In the analysis of immune cell subpopulation difference, the non-parametric Mann-Whitney U-test (significance threshold $p<0.05$) was used to compare the immune infiltration scores of the training set between groups, and the immune cell subpopulations with significant differences were screened out. Spearman rank correlation analysis was performed on the differential cells by R software package psych (2.4.6.26) (threshold setting: $|r|> 0.3$ and $p< 0.05$), an immune cell interaction network was constructed (Fig. 5B, C, F, G).

Spearman correlation analysis further revealed the functional relationship between biomarkers (ZCCHC2, TNFS-

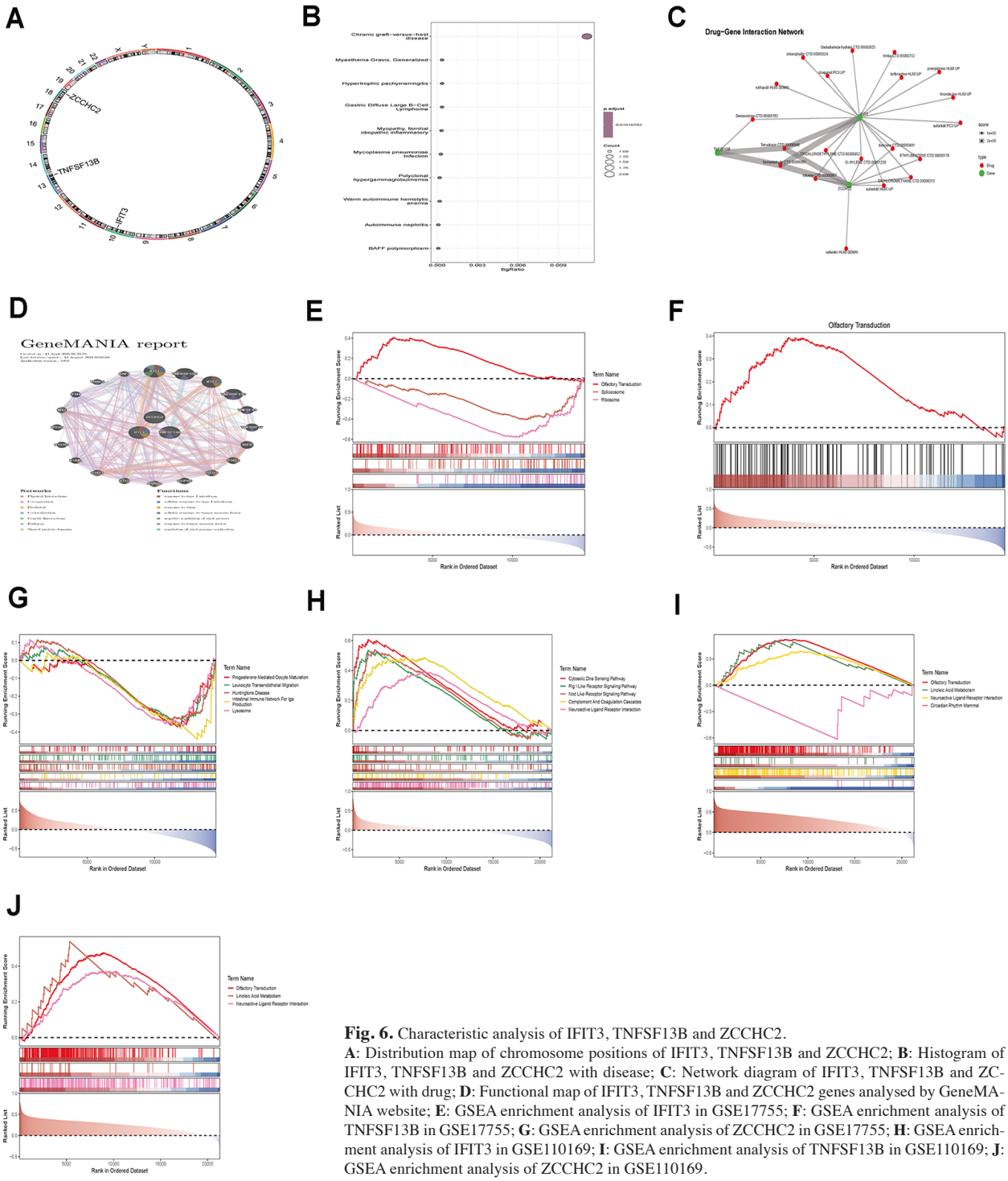

Fig. 6. Characteristic analysis of IFIT3, TNFSF13B and ZCCHC2.
A: Distribution map of chromosome positions of IFIT3, TNFSF13B and ZCCHC2; **B**: Histogram of IFIT3, TNFSF13B and ZCCHC2 with disease; **C**: Network diagram of IFIT3, TNFSF13B and ZCCHC2 with drug; **D**: Functional map of IFIT3, TNFSF13B and ZCCHC2 genes analysed by GeneMANIA website; **E**: GSEA enrichment analysis of IFIT3 in GSE17755; **F**: GSEA enrichment analysis of TNFSF13B in GSE17755; **G**: GSEA enrichment analysis of ZCCHC2 in GSE17755; **H**: GSEA enrichment analysis of IFIT3 in GSE110169; **I**: GSEA enrichment analysis of TNFSF13B in GSE110169; **J**: GSEA enrichment analysis of ZCCHC2 in GSE110169.

F13B, IFIT3) and differential immune cells (Fig. 5D, H). Notably, the proinflammatory factor TNFSF13B was significantly positively correlated with the degree of macrophage infiltration in RA patients, while the interferon-inducible gene IFIT3 was strongly negatively correlated with plasmacytoid dendritic cells in SLE patients (Fig. 5D, H). These findings suggest that different biomarkers may be involved in disease development through specific regulation of specific immune cell subsets.

Characterisation of IFIT3, TNFSF13B and ZCCHC2

Chromosomal localisation of genes is of great significance to the study of gene structure, function and interaction. In order to explore the chromosomal localisation of biomarkers, RCircos (1.2.2) was used to visualise their chromosomal localisation. IFIT3 gene is clearly mapped on chromosome 10, TNFSF13B gene on chromosome 13, and ZCCHC2 gene on chromosome 13 (Fig. 6A).

Network analysis based on the DisGeNET database revealed that TNFSF13B as a core biomarker was associated with Chronic graft-versus-host

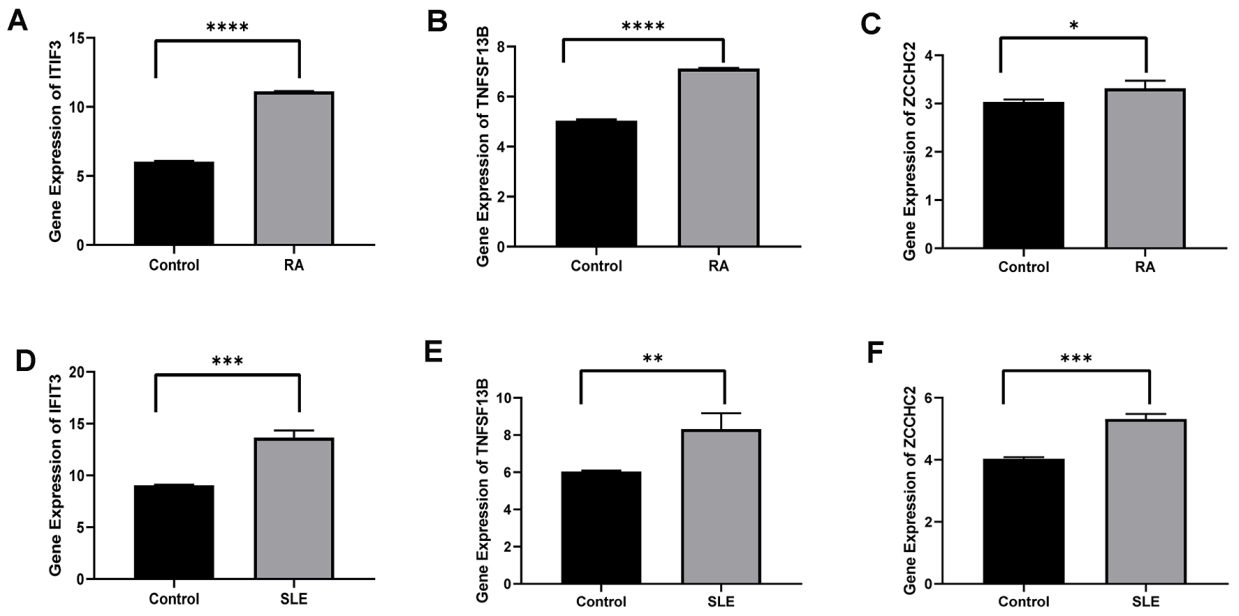

Fig. 7. RT-QPCR experimental validation.
A: IFIT3 expression level in RA samples; **B**: TNFSF13B expression level in RA samples; **C**: ZCCHC2 expression level in RA samples; **D**: IFIT3 expression level in SLE samples; **E**: TNFSF13B expression level in SLE samples; **F**: ZCCHC2 expression level in SLE samples.
Note: * indicates adj.*p*-value <0.05, ** indicates adj.*p*-value <0.01, *** indicates adj.*p*-value <0.001, **** indicates adj.*p*-value <0.0001.

disease, Polyclonal hypergammaglobulaemia, Warm autoimmune haemolytic anaemia and autoimmune neuropathy, and IFIT3 was associated with Chronic graft-versus-host disease, suggesting its pivotal role in multisystem diseases and potential for cross-disease therapeutic targeting (Fig. 6B).

In order to explore drugs that may target biomarkers, the Drug-Gene Interaction Database was used to predict potential drugs or compounds associated with biomarkers, and ggplot2 was used for visualisation. Here, IFIT3, TNFSF13B and ZCCHC2 were used as a set to find common targets for drug enrichment analysis, so the top two drugs with the highest enrichment scores were formaldehyde and tetratoxin (Fig. 6C).

GeneMANIA includes the functions of IFIT3 and TNFSF 13B, IFIT3 is related to response to type I interferon, cellular response to type I interferon and response to virus, TNFSF 13B is related to cellular response to tumour necrosis factor (Fig. 6D).

In order to explore the functional association of biomarkers (IFIT3, TNFSF13B, ZCCHC2) in RA and SLE, we calculated the co-expression profiles of biomarkers and other genes by Spearman correlation analysis based on transcriptome data of training set samples, and then performed gene set enrichment analysis (GSEA) after sorting according to correlation coefficients. The results showed that these genes were significantly enriched in pathways associated with immune regulation and inflammation (Fig. 6E-J).

In RA dataset (GSE17755), high expression of IFIT3 was positively correlated with olfactory transduction pathway, suggesting that IFIT3 may be involved in sensory neuron-mediated inflammatory signalling (Fig. 6E). In SLE dataset GSE110169, IFIT3 is enriched in the cytoplasmic DNA sensing pathway and RIG-I like receptor signalling pathway, suggesting that it activates the type I interferon response by recognising viral nucleic acids. In addition, IFIT3 was also significantly enriched in the Complement and Coagulation Cascades in the SLE dataset (GSE110169), further supporting its central role in innate immunity (Fig. 6H).

TNFSF13B is associated with olfactory transduction pathway in RA and SLE, suggesting that TNFSF13B may be involved in sensory neuron-mediated inflammatory signal transduction (Fig. 6F, I). ZCCHC2 is significantly associated with progesterone mediated oocyte maturation and Huntington's disease pathways in RA, suggesting that it may be involved in the intersection of cell cycle regulation and neurodegeneration (Fig. 6G). In SLE, ZCCHC2 is enriched in olfactory transduction pathway, suggesting that ZCCHC2 may be involved in sensory neuron-mediated inflammatory signal transduction (Fig. 6J).

RT-QPCR experimental verification

In an inter-group comparison of gene expression levels, mRNA expression of IFIT3, TNFSF13B and ZCCHC2 was significantly higher in both RA and SLE groups than in healthy controls (Fig. 7A-F). Specifically, IFIT3 was significantly upregulated in both RA and SLE groups, and the expression level of SLE group was significantly higher than RA group (Fig. 7A, D); TNFSF13B was also significantly upregulated in RA and SLE groups (Fig. 7B, E); and ZCCHC2 was significantly upregulated in RA and SLE groups (Fig. 7C, F). These results suggest that although the three genes are synergistically abnormal in both diseases, their up-regulation is more significant in SLE, and TNFSF13B and IFIT3 may have more prominent pathological significance in SLE, while the difference in ZCCHC2 may be regulated by other factors.

Discussion

By integrating transcriptome data and machine learning screening, this study systematically revealed the potential co-disease association between RA and SLE in molecular mechanism and verified the expression characteristics of key genes (IFIT3, TNFSF13B, ZCCHC2) and their clinical significance. These findings not only provide new insights into understanding the similarities and differences between RA and SLE, but also lay the foundation for developing diagnostic markers and therapeutic targets across diseases.

Molecular mechanisms of shared genes and disease similarities and differences

The co-upregulation of IFIT3, TNFSF13B and ZCCHC2 in RA and SLE suggests that these two diseases may drive pathological processes through partially shared molecular pathways such as innate immune response and B cell activation. In SLE, IFIT3 acts as an interferon-inducible protein and is closely related to the type I interferon signalling pathway. IFIT3 was found to be significantly upregulated in peripheral blood mononuclear cells (PBMCs) of SLE patients and strongly correlated with anti-dsDNA antibody titres, suggesting that IFIT3 is involved in autoantibody formation through interferon pathway (26, 27). IFIT3 also promotes IFNα production through cGAS-STING pathway, exacerbating immune dysregulation in SLE (27). In RA, IFIT3 expression is moderately correlated with CRP levels and may be indirectly involved in synovial inflammation via Toll-like receptor (TLR) signalling pathways (26, 28). The TLR4/NF-ϰB pathway is activated in RA and promotes the release of inflammatory factors such as IL-6 and IL-17, and IFIT3 may affect the pathological process of RA by regulating this pathway (29, 30).

TNFSF13B encodes B cell activating factor (BAFF), which is highly expressed in RA and SLE. BAFF plays a central role in both diseases by promoting B cell activation and autoantibody production (31). Activation of TLR signalling pathways, such as TLR9, induces BAFF expression, further driving B cell-mediated autoimmune responses (32, 33).

Current research does not directly support a functional role for ZCCHC2 in RA and SLE, but the expression changes of other members of the ZCCHC family (such as ZCCHC6/ZCCHC11) in SLE suggest that the family may be involved in immune regulation (11,34-36). Further investigation should focus on whether ZCCHC2 affects the pathological process of RA or SLE through similar mechanisms (such as RNA modification, inflammatory signalling pathway).

Clinical significance and diagnostic value of gene expression

TNFSF13B as a core regulatory factor of B cell activation, its high AUC value in the diagnosis of RA and SLE may be related to HLA gene association analysis. Some studies have pointed out that HLA-DQA1, DQB1 and other HLA-II alleles are associated with SLE and RA. Genes with high predictive performance have been screened by machine learning models, suggesting that HLA genes may affect disease progression through B cell activation pathway (37). More significant differences in IFIT3 expression in SLE may be associated with activation of interferon signalling pathway, and some studies have pointed out that gene set enrichment analysis shows that IFIT3 gene is significantly enriched in interferon signalling pathway and correlated with disease activity (38, 39). Deng *et al*. screened interferon-related genes (IFI44, IFIT3) through machine learning, and their AUC values reached 0.753 in SLE, verifying the central role of interferon signal in SLE (40). The intergroup differences in ZCCHC2 are not significant, which may reflect its indirect regulation by disease-specific regulatory networks. Studies have identified zinc finger protein genes associated with RA phenotypes through LASSO regression and random forest algorithms, and validated a nomogram model to assess their diagnostic value (41).

Correlation between immune cell infiltration and gene function

Immunocyte infiltration analysis further revealed differences in immune microenvironment between RA and SLE. Macrophage activation in RA synovial microenvironment is a key driver of inflammation persistence. Tian *et al*. noted that macrophages significantly infiltrate the synovium of RA patients and exacerbate synovial destruction by releasing pro-inflammatory factors such as TNF-α, IL-1β (42). Pabon-Porras *et al*. further emphasised that the innate immune system (including macrophages) not only initiates an early inflammatory response in RA, but also maintains disease progression through continued activation (43). Although TNFSF13B is not directly related to macrophage infiltration in RA, the proinflammatory mechanism of macrophage activation is consistent with the functional direction of TNFSF13B, which may indirectly affect the inflammatory microenvironment by regulating the interaction between macrophages and other immune cells.

IFIT3 promotes the production of type I interferon (IFN) and other proinflammatory cytokines by enhancing the activity of cGAS/STING signalling pathway. Experiments have shown that knocking down IFIT3 significantly reduces virus-induced IFNβ expression, while overexpression of IFIT3 enhances this process. IFIT3 directly interacts with STING and TANK binding kinase 1 (TBK1) to further activate downstream signals, thereby exacerbating inflammatory responses in SLE patients' monocytes (44). This mechanism is considered an important molecular basis for the onset of SLE, although there is no direct evidence in current studies proving that IFIT3 functions through the immune microenvironment in SLE. As an interferon-induced gene, IFIT3 may inhibit the secretion of IFN-α by pDCs through a negative feedback mechanism, which is consistent with the dysregulation of the interferon pathway observed in SLE.

Limitations and future directions

Despite this study revealing potential comorbidity mechanisms between RA and SLE through multi-omics analysis and machine learning methods, limitations still exist. First, the heterogeneity of public datasets (such as differences

in sample sources and definitions of disease activity) may affect the generalisability of the results, a point that has been widely discussed in multi-omics studies of rheumatology (45). Secondly, the lack of direct comparisons of Rhupus syndrome (RA-SLE overlap syndrome) limits the in-depth exploration of comorbidity-specific mechanisms, which have already shown their importance in clinical settings (46).

Future research can be advanced in the following directions:

1. Functional verification, through cell experiments or animal models to explore the regulation of IFIT3 on interferon signals and the influence of TNFSF13B on B cell differentiation, the mechanism is closely related to Th17/Treg balance;
2. Environmental-gene interaction, analysis of halogenated compounds such as dichloromethane and ZCCHC2; The relationship between expression, explore the role of epigenetic modification in disease;
3. Clinical transformation, expand the cohort size and combine protein detection to optimise the prediction model, as shown in the RA/SLE co-treatment strategy;
4. Research on the mechanism of co-disease, including Rhupus patient samples to clarify the regulatory network differences between shared genes and specific genes, Such studies have preliminarily revealed its unique molecular characteristics;
5. Due to the characteristics of exploratory research, this study did not conduct *a priori* power analysis, which may affect the interpretation of negative results and suggests that these findings be further validated through multicentre large sample studies in the future.

Conclusion

This study elucidates the molecular mechanisms of RA/SLE comorbidity, identifies cross-disease biomarkers and their interactions with immune cells and drugs, providing theoretical basis for precision diagnosis and treatment. The study limitations include data heterogeneity and the lack of Rhupus patient samples, which need to be validated through functional experiments and multicentre cohorts in the future.

Acknowledgements

We are grateful for the support from Gansu Province Natural Science Foundation (grant no. 21JR1RA173) and Lanzhou Science and Technology Project (grant no. 2020-ZD-90).

References

1. MONTALBAN X, WALLACE D, GENOVESE MC *et al*.: A plain language summary of what clinical studies can tell us about the safety of evobrutinib - a potential treatment for multiple sclerosis. *Neurodegener Dis Manag* 2023; 13(4): 207-13. https://doi.org/10.2217/nmt-2023-0003
2. VIDAL ALEJANDRE B, TOVAR SUGRANES E, LOPEZ POZA R, ANDRES M, MARTINEZ-VIDAL MP: Human papiloma virus screening: evaluation of testing and surveillance in rheumatoid arthritis, psoriatic arthritis and systemic lupus erythematosus. *Reumatol Clin* (Engl Ed) 2020. https://doi.org/10.1016/j.reuma.2020.05.007
3. MUTALIPOVA G, BEKARYSSOVA D, YESSIRKEPOV M, BEKARISSOVA S: Trends and gender disparities in the incidence of rheumatic diseases: a regional study from 2018 to 2021. *Rheumatol Int* 2024; 44(12): 2847-51. https://doi.org/10.1007/s00296-024-05725-y
4. YANG M, ZHENG H, SU Y *et al*.: Bioinformatics analysis identified the hub genes, mRNA-miRNA-lncRNA axis, and signaling pathways involved in rheumatoid arthritis Pathogenesis. *Int J Gen Med* 2022; 15: 3879-93. https://doi.org/10.2147/ijgm.s353487
5. WU R, LONG L, ZHOU Q, SU J, SU W, ZHU J: Identification of hub genes in rheumatoid arthritis through an integrated bioinformatics approach. *J Orthop Surg Res* 2021; 16(1): 458. https://doi.org/10.1186/s13018-021-02583-3
6. ZHOU S, LU H, XIONG M: Identifying immune cell infiltration and effective diagnostic biomarkers in rheumatoid arthritis by bioinformatics analysis. *Front Immunol* 2021; 12: 726747. https://doi.org/10.3389/fimmu.2021.726747
7. LU H, ZHANG J, JIANG Z *et al*.: Detection of genetic overlap between rheumatoid arthritis and systemic lupus erythematosus using GWAS summary statistics. *Front Genet* 2021; 12: 656545. https://doi.org/10.3389/fgene.2021.656545
8. REN C, LI M, DU W *et al*.: Comprehensive bioinformatics analysis reveals hub genes and inflammation state of rheumatoid arthritis. *Biomed Res Int* 2020; 2020: 6943103. https://doi.org/10.1155/2020/6943103
9. WANG J, XUE Y, ZHOU L: New classification of rheumatoid arthritis based on immune cells and clinical characteristics. *J Inflamm Res* 2024; 17: 3293-305. https://doi.org/10.2147/jir.s395566
10. RESENDE ABL, MONTEIRO GP, RAMOS CC, LOPES GS, BROEKMAN LA, DE SOUZA JM: Integrating the autoimmune connective tissue diseases for the medical student: a classification proposal based on pathogenesis and clinical phenotype. *Heliyon* 2023; 9(6): e16935. https://doi.org/10.1016/j.heliyon.2023.e16935
11. DOUDAR NA, KHATTAB R, QURANY EA, REYAD HR, MOSTAFA N: Interleukin 1 receptor associated kinase 1 gene polymorphism association with risk of rheumatological diseases in Egyptian population. *Mol Biol Rep* 2025; 52(1): 135. https://doi.org/10.1007/s11033-025-10223-w
12. FAN F, LIU S, WANG B, SONG X, WANG W: Integrated analyses uncover new features of atypical memory B cells and novel targets for intervention. *Immunobiology* 2025; 230(2): 152877. https://doi.org/10.1016/j.imbio.2025.152877
13. TYAGI N, MEHLA K, GUPTA D: Deciphering novel common gene signatures for rheumatoid arthritis and systemic lupus erythematosus by integrative analysis of transcriptomic profiles. *PLoS One* 2023; 18(3): e0281637. https://doi.org/10.1371/journal.pone.0281637
14. XU Q, ZHANG X, GE S, XU C, LV Y, SHUAI Z: Triptoquinone A and B exercise a therapeutic effect in systemic lupus erythematosus by regulating NLRC3. *PeerJ* 2023; 11: e15395. https://doi.org/10.7717/peerj.15395
15. DRIE T, KHALAYLI N, HAIDAR G, HAJ ALI D: Rhupus syndrome. a case report of a rare combination. *Ann Med Surg* (Lond) 2024; 86(1): 535-38. https://doi.org/10.1097/ms9.0000000000001517
16. CHEN X, LI Y, CHEN X, LIU Y, XIE J, GUO D: Rhupus syndrome: a unique disease overlapping systemic lupus erythematosus and rheumatoid arthritis. *Arch Dermatol Res* 2024; 317(1): 127. https://doi.org/10.1007/s00403-024-03610-z
17. UPADHYAYA S, AGARWAL M, UPADHYAYA A, PATHANIA M, DHAR M: Rhupus syndrome: a diagnostic dilemma. *Cureus* 2022; 14(9): e29018. https://doi.org/10.7759/cureus.29018
18. ANTONINI L, LE MAUFF B, MARCELLI C, AOUBA A, DE BOYSSON H: Rhupus: a systematic literature review. *Autoimmun Rev* 2020; 19(9): 102612. https://doi.org/10.1016/j.autrev.2020.102612
19. LIU X, LI B, LIN Y *et al*.: Exploring the shared gene signatures and mechanism among three autoimmune diseases by bulk RNA sequencing integrated with single-cell RNA sequencing analysis. *Front Mol Biosci* 2024; 11: 1520050. https://doi.org/10.3389/fmolb.2024.1520050
20. SHEN N, ZHANG Y, DING Z *et al*.: Predicting intraoperative blood loss risk in severe lumbar disc herniation patients undergoing PLIF: a multicenter cohort study using ensemble learning. *Int J Surg* 2025; 111(9): 5904-13. https://doi.org/10.1097/js9.0000000000002730
21. WEI H, SUN J, SHAN W *et al*.: Environmental chemical exposure dynamics and machine learning-based prediction of diabetes mellitus. *Sci Total Environ* 2022; 806(Pt 2): 150674. https://doi.org/10.1016/j.scitotenv.2021.150674
22. WARKENTIN MT, AL-SAWAIHEY H, LAM S *et al*.: Radiomics analysis to predict pulmonary nodule malignancy using machine learning approaches. *Thorax* 2024; 79(4): 307-15. https://doi.org/10.1136/thorax-2023-220226
23. DING DY, LI S, NARASIMHAN B, TIBSHIRANI

R: Cooperative learning for multiview analysis. *Proc Natl Acad Sci USA* 2022; 119(38). https://doi.org/10.1073/pnas.2202113119
24. OUYANG W, LAI Z, HUANG H, LING L: Machine learning-based identification of cuproptosis-related lncRNA biomarkers in diffuse large B-cell lymphoma. *Cell Biol Toxicol* 2025; 41(1): 72. https://doi.org/10.1007/s10565-025-10030-w
25. LIAO LD, FERRARA A, GREENBERG MB *et al*.: Development and validation of prediction models for gestational diabetes treatment modality using supervised machine learning: a population-based cohort study. *BMC Med* 2022; 20(1): 307. https://doi.org/10.1186/s12916-022-02499-7
26. JIAN S, LI H: Peripheral mononuclear cells and systemic lupus erythematosus association: Integrated study of single-cell sequencing and mendelian randomization analysis. *Lupus* 2024; 33(14): 1526-37. https://doi.org/10.1177/09612033241292705
27. KUGA T, CHIBA A, MURAYAMA G *et al*.: Enhanced GATA4 expression in senescent systemic lupus erythematosus monocytes promotes high levels of IFNalpha production. *Front Immunol* 2024; 15: 1320444. https://doi.org/10.3389/fimmu.2024.1320444
28. LI H, WANG T, LI B *et al*.: Bioinformatic analysis of immune-related transcriptome affected by IFIT1 gene in childhood systemic lupus erythematosus. *Transl Pediatr* 2023; 12(8): 1517-26. https://doi.org/10.21037/tp-23-365
29. TANG J, YU Z, XIA J *et al*.: METTL14-mediated m6A modification of TNFAIP3 involved in inflammation in patients with active rheumatoid arthritis. *Arthritis Rheumatol* 2023; 75(12): 2116-29. https://doi.org/10.1002/art.42629
30. YU C, WANG D, YANG Z, WANG T: Pharmacological effects of polyphenol phytochemicals on the intestinal inflammation via targeting TLR4/NF-kappaB signaling pathway. *Int J Mol Sci* 2022; 23(13): https://doi.org/10.3390/ijms23136939
31. WANG Y, BAO L, LIU M *et al*.: The role of the toll-like receptor signaling pathway in autoimmune diseases and treatment with traditional Chinese medicine: a literature review. *Endocr Metab Immune Disord Drug Targets* 2025 Jan 21. https://doi.org/10.2174/0118715303340093241227094242
32. LV J, WEI Y, YIN JH *et al*.: The tumor immune microenvironment of nasopharyngeal carcinoma after gemcitabine plus cisplatin treatment. *Nat Med* 2023; 29(6): 1424-36. https://doi.org/10.1038/s41591-023-02369-6
33. GU C, HUANG Z, SUN Y *et al*.: Characterization of human immortalized keratinocyte cells infected by monkeypox virus. *Viruses* 2024; 16(8): 10.3390/v16081206
34. LIN Z, LI P, WANG C, TAN H: Functional characterization of SLC2A3 in rheumatoid arthritis: unraveling its role in ferroptosis and inflammatory pathways. *Int J Rheum Dis* 2024; 27(12): e70009. https://doi.org/10.1111/1756-185x.70009
35. XU L, WANG H, SUN C *et al*.: GZMK facilitates experimental rheumatoid arthritis progression by interacting with CCL5 and activating the ERK signaling. *Inflammation* 2025; 48(4): 1940-56. https://doi.org/10.1007/s10753-024-02166-4
36. CHEN W, FANG Y, WANG H *et al*.: Role of chemokine receptor 2 in rheumatoid arthritis: a research update. *Int Immunopharmacol*. 2023; 116: 109755. https://doi.org/10.1016/j.intimp.2023.109755
37. CHUNG CW, HSIAO TH, HUANG CJ *et al*.: Machine learning approaches for the genomic prediction of rheumatoid arthritis and systemic lupus erythematosus. *BioData Min* 2021; 14(1): 52. https://doi.org/10.1186/s13040-021-00284-5
38. OUYANG G, WU Z, LIU Z *et al*.: Identification and validation of potential diagnostic signature and immune cell infiltration for NAFLD based on cuproptosis-related genes by bioinformatics analysis and machine learning. *Front Immunol* 2023; 14: 1251750. https://doi.org/10.3389/fimmu.2023.1251750
39. CHEN W, LI ZY, HUANG L *et al*.: Integrative bioinformatics analysis identifies ddx60 as a potential biomarker for systemic lupus erythematosus. *Dis Markers* 2023; 2023: 8564650. https://doi.org/10.1155/2023/8564650
40. DENG Y, ZHOU Y, SHI J *et al*.: Potential genetic biomarkers predict adverse pregnancy outcome during early and mid-pregnancy in women with systemic lupus erythematosus. *Front Endocrinol* (Lausanne) 2022; 13: 957010. https://doi.org/10.3389/fendo.2022.957010
41. LONG X, ZENG H, ZHANG Y, LU Q, CAO Z, SHU H: Development of a reliable GADSAH model for differentiating AFP-negative hepatic benign and malignant occupying lesions. *J Hepatocell Carcinoma* 2024; 11: 607-68. https://doi.org/10.2147/jhc.s452628
42. TIAN X, CHEN J, HONG Y, CAO Y, XIAO J, ZHU Y: Exploring the role of macrophages and their associated structures in rheumatoid arthritis. *J Innate Immun* 2025; 17(1): 95-111. https://doi.org/10.1159/000543444
43. PABON-PORRAS MA, MOLINA-RIOS S, FLOREZ-SUAREZ JB, CORAL-ALVARADO PX, MENDEZ-PATARROYO P, QUINTANA-LOPEZ G: Rheumatoid arthritis and systemic lupus erythematosus: Pathophysiological mechanisms related to innate immune system. *SAGE Open Med* 2019; 7. https://doi.org/10.1177/2050312119876146
44. WANG J, DAI M, CUI Y *et al*.: Association of abnormal elevations in IFIT3 with overactive cyclic GMP-AMP synthase/stimulator of interferon genes signaling in human systemic lupus erythematosus monocytes. *Arthritis Rheumatol* 2018; 70(12): 2036-45. https://doi.org/10.1002/art.40576
45. LI ZF, WU X, WU LJ *et al*.: [Clinical features of patients with Rhupus syndrome]. *Beijing Da Xue Xue Bao Yi Xue Ban* 2021; 53(5): 933-37. https://doi.org/10.19723/j.issn.1671-167x.2021.05.020
46. BHATTACHARYYA S, HELFGOTT SM: Neurologic complications of systemic lupus erythematosus, sjogren syndrome, and rheumatoid arthritis. *Semin Neurol* 2014; 34(4): 425-36. https://doi.org/10.1055/s-0034-1390391